

Article

# The Extreme Values of Young's Modulus and the Negative Poisson's Ratios of Rhombic Crystals

Valentin A. Gorodtsov  and Dmitry S. Lisovenko \* 

Ishlinsky Institute for Problems in Mechanics RAS, Prosp. Vernadskogo 101-1, 119526 Moscow, Russia; gorod@ipmnet.ru

\* Correspondence: lisovenko@ipmnet.ru

**Abstract:** The extreme values of Young's modulus for rhombic (orthorhombic) crystals using the necessary and sufficient conditions for the extremum of the function of two variables are analyzed herein. Seven stationary expressions of Young's modulus are obtained. For three stationary values of Young's modulus, simple analytical dependences included in the sufficient conditions for the extremum of the function of two variables are revealed. The numerical values of the stationary and extreme values of Young's modulus for all rhombic crystals with experimental data on elastic constants from the well-known Landolt-Börnstein reference book are calculated. For three stationary values of Young's modulus of rhombic crystals, a classification scheme based on two dimensionless parameters is presented. Rhombic crystals ((CH<sub>3</sub>)<sub>3</sub>NCH<sub>2</sub>COO·(CH)<sub>2</sub>(COOH)<sub>2</sub>, I, SC(NH<sub>2</sub>)<sub>2</sub>, (CH<sub>3</sub>)<sub>3</sub>NCH<sub>2</sub>COO·H<sub>3</sub>BO<sub>3</sub>, Cu-14 wt%Al, 3.0wt%Ni, NH<sub>4</sub>B<sub>5</sub>O<sub>8</sub>·4H<sub>2</sub>O, NH<sub>4</sub>HC<sub>2</sub>O<sub>4</sub>·1/2H<sub>2</sub>O, C<sub>6</sub>N<sub>2</sub>O<sub>3</sub>H<sub>6</sub> and CaSO<sub>4</sub>) having a large difference between maximum and minimum Young's modulus values were revealed. The highest Young's modulus among the rhombic crystals was found to be 478 GPa for a BeAl<sub>2</sub>O<sub>4</sub> crystal. More rigid materials were revealed among tetragonal (PdPb<sub>2</sub>; maximum Young's modulus, 684 GPa), hexagonal (graphite; maximum Young's modulus, 1020 GPa) and cubic (diamond; maximum Young's modulus, 1207 GPa) crystals. The analytical stationary values of Young's modulus for tetragonal, hexagonal and cubic crystals are presented as special cases of stationary values for rhombic crystals. It was found that rhombic, tetragonal and cubic crystals that have large differences between their maximum and minimum values of Young's modulus often have negative minimum values of Poisson's ratio (auxetics). We use the abbreviated term auxetics instead of partial auxetics, since only the latter were found. No similar relationship between a negative Poisson's ratio and a large difference between the maximum and minimum values of Young's modulus was found for hexagonal crystals.



**Citation:** Gorodtsov, V.A.; Lisovenko, D.S. The Extreme Values of Young's Modulus and the Negative Poisson's Ratios of Rhombic Crystals. *Crystals* **2021**, *11*, 863. <https://doi.org/10.3390/cryst11080863>

Academic Editor: Alberta Ferrarini

Received: 4 May 2021

Accepted: 22 July 2021

Published: 25 July 2021

**Publisher's Note:** MDPI stays neutral with regard to jurisdictional claims in published maps and institutional affiliations.



**Copyright:** © 2021 by the authors. Licensee MDPI, Basel, Switzerland. This article is an open access article distributed under the terms and conditions of the Creative Commons Attribution (CC BY) license (<https://creativecommons.org/licenses/by/4.0/>).

**Keywords:** rhombic crystals; Young's modulus; elasticity; crystals; auxetics

## 1. Introduction

Anisotropic materials occupy an important place in modern technical applications. While the description of the linear elastic properties of isotropic media requires only two independent elastic constants, the number of important elastic constants increases with decreasing symmetry of materials. The deformation of anisotropic crystalline bodies depends not only on the locations of external forces in relation to the body, but also on the orientation of the crystallographic axes inside it. In addition, restrictions on such important elastic engineering characteristics (combinations of elastic constants), such as Young's moduli, Poisson's ratios and shear moduli, are reduced. In particular, if Poisson's ratios in isotropic media have restrictions of  $-1$  below and  $0.5$  above, then for crystals of all seven symmetry systems, including the most symmetric cubic system, there are no general restrictions on the values and signs of Poisson's ratios [1].

An analysis of the variability of Poisson's ratios and Young's moduli of a large number of real crystals of all seven crystal systems (cubic, hexagonal, rhombohedral, tetragonal, rhombic, monoclinic and triclinic) was carried out in [2,3], based on extensive information

on experimental elastic constants in the Landolt–Börnstein reference book [4]. In [2], the extrema of Poisson's ratios and correlations of the extrema with the values of elastic anisotropy indices, generalizing the classical Zener exponent, were found. The extrema of Poisson's ratios, together with the extrema of Young's moduli, were also established for real crystals of all crystalline systems in [3], limited to a one-parameter set of orientations. General analytical results for the extrema of the basic engineering moduli of materials of any crystal symmetry were obtained in [5–7]. In [6], the stationary values and extrema of Young's modulus and shear modulus were analyzed. In [7], conditions for the stationary values, maxima and minima of the three engineering moduli of anisotropic elastic materials were derived.

Several studies have been devoted to the analysis of the extreme values of Young's modulus and Poisson's ratio for crystals of some particular symmetry systems and examples of real crystals. In [8], a variational Lagrangian analysis of the extrema of Young's modulus for cubic and hexagonal crystals was supplemented with examples of classifications and results for some crystals. In [9], general expressions for the extrema of Young's moduli of six constant tetragonal crystals were established, and results were given for many materials. In [10,11], analytical expressions for the extreme values of Poisson's ratio for cubic crystals were obtained. These analytical relationships were used to calculate the extreme values of known crystals. It has been demonstrated that high absolute values of the extrema of Poisson's ratio can be observed for specific orientations of some crystals. In [10], indium–thallium alloys were such crystals. In [11], most of their attention was paid to metastable cubic metal alloys and analyzing of the role of the elastic anisotropy coefficient, which vanishes in the limit of an isotropic medium. Stationary and extreme values of Young's moduli and Poisson's ratios for hexagonal crystals were established in [12] based on an analytical analysis of the angular orientations of crystals and several dimensionless anisotropy characteristics that disappear in the isotropic limit. Numerical results were obtained on the basis of 147 hexagonal crystals. The anisotropy coefficients made it possible to construct classification schemes for the distributions of the extrema of Young's modulus and Poisson's ratio of real crystals.

The history of materials with negative Poisson's ratio dates back to the publication on crystalline pyrite in the well-known monograph by A.E.H. Love [13]. Experimental research and qualitative analysis by R.S. Lakes of negative Poisson's ratios for metal and polymer foams [14,15] had a great influence on further studies of various materials and designs. The proposal by K.E. Evans of replacing the longer phrase “negative-Poisson's-ratio materials” with the term auxetics [16,17] has become generally accepted.

The first theoretical studies of auxetics by K.W. Wojciechowski [18,19] dealt with a 2D isotropic lattice built from 2D anisotropic molecules. In [20], Tretiakov K.V. and Wojciechowski K.W. studied the features of the formation of auxetics in the isotropic 2D solid phase depending on the 2D molecular geometry. In [21], the same authors analyzed the formation of auxetics, partially auxetics and nonauxetics among 2D crystals of five crystal systems with anisotropic 2D molecules in the form of rigid cyclic tetramers. In the article by K.W. Wojciechowski and A.C. Branka [22], approximations of free volume and Monte Carlo simulation revealed the decisive role of the hexagonal shape of the molecule in the 2D isotropic lattice model, which leads to auxeticity due to mirror symmetry breaking (chirality). However, in [23], K.W. Wojciechowski demonstrated that a 2D isotropic model with 2D anisotropic molecules such as cyclic trimers can form a nonchiral phase with a negative Poisson's ratio.

A new series of studies by K.W. Wojciechowski, K.V. Tretiakov, J.W. Narojczyk, P.M. Piglowski and their collaborators has concerned the auxeticity of 3D model materials with 2D thin layers and 1D narrow channels (“nanolayers” and “nanochannels”) [24–32]. The auxetic properties of the composites of spherical particles in some main matrix and nanochannels [24,25,28–30] or nanolayers [26,27,31] depended on their orientations, relative particle diameters and filling densities. It was shown in [32] that the orthogonal

combination of nanochannels and nanolayers can lead, with a sufficiently large size of spherical inclusions, to the absence of auxetic properties of the composite.

Another line of research into the mechanism of auxeticity was undertaken by J.N. Grima, K.E. Evans and A. Alderson et al. [33–58]. The concepts of the mechanism of auxeticity of materials in these articles were based on rotations of simplified 2D geometric structures from triangular, square, rectangular and rhombic forms (etc.). Following A. Alderson and K.E. Evans, the auxetic nature of the deformation of a number of crystals (zeolites, silicates,  $\alpha$ -cristobalite and  $\beta$ -cristobalite in particular) was associated with rotation and dilation of 3D tetrahedral and rotating 3D cuboidal microstructures [59–68]. It was shown in [69] that the auxeticity and negative linear compressibility of Boron Arsenate arise mainly due to deformations of framework tetrahedra. In [70], the manifestation of auxeticity and negative linear compressibility was discussed in the case of the formation of a 3D microstructure of a metamaterial due to stretching in out-of-plane direction of the original 2D “rotating squares”. In [71], the possibility of auxeticity for a broad range of loading directions and negative linear compressibility for a small number of such directions was discussed for a 3D metamaterial composed of arrowhead-like structural units. In [72], the role of the rearrangement of the 3D microstructure of boron arsenite under shear deformation in auxeticity and negative linear compressibility was discussed. An important feature of the shearing deformation of tetrahedra on the projection planes is the distortion of the rotating squares.

Auxetic materials are often found among natural anisotropic materials. There are particularly many of them (about three hundred) among highly symmetric cubic crystals [73–103]. Since the negativity of Poisson’s ratio usually corresponds to the selected directions of crystal orientation [7,11], in this case we actually focus on partial auxetics. Fewer auxetics are found among crystals of lower symmetry.

In this article, we consider the problem of stationary and extreme values of Young’s modulus, and the question of the relationship between the extrema of Young’s modulus and the value and sign of Poisson’s ratio. Section 2 begins with a presentation of Young’s modulus versus crystal orientation angles. Then six anisotropy coefficients are introduced as linear combinations of the compliance triples that disappear in the isotropic limit. Anisotropy coefficients for 18 crystals are shown in Table 1. A more complete list is provided in the Supplemental Material. In Section 3, the analysis of the second derivatives made it possible to find the extrema of Young’s modulus for 140 rhombic crystals, shown partially in Table 2 and completely in the Supplementary Material. The dependence of three stationary values of Young’s modulus on the anisotropy coefficients is presented in the form of a classification scheme. An analysis of the extrema of Poisson’s ratios showed that more than 50 rhombic crystals are auxetic; about 30 of them correspond to the ratio  $E_{\max}/E_{\min} > 3$  (Table 3 and Supplementary Material). In Section 4, the stationary values of Young’s modulus for cubic, hexagonal and tetragonal crystals are discussed briefly as special cases of the rhombic system. In Section 5, conclusions are given.

**Table 1.** Values of anisotropy coefficients  $\Delta_1$ ,  $\Delta_2$ ,  $\Delta_3$ ,  $\Delta_4$ ,  $\Delta_5$  and  $\Delta_6$  of some rhombic crystals.

Crystals	$\Delta_1,$ TPa <sup>−1</sup>	$\Delta_2,$ TPa <sup>−1</sup>	$\Delta_3,$ TPa <sup>−1</sup>	$\Delta_4,$ TPa <sup>−1</sup>	$\Delta_5,$ TPa <sup>−1</sup>	$\Delta_6,$ TPa <sup>−1</sup>
CaSO <sub>4</sub>	−42.2	−47.5	−6.57	−8.02	−8.16	−4.33
CaCO <sub>3</sub>	−1.71	4.54	−13.0	−7.73	3.48	2.48
BaMnF <sub>4</sub> , s <sup>E</sup>	−9.2	1.1	17.4	33.9	12.9	19.1
Cs <sub>2</sub> SO <sub>4</sub>	2.6	4.4	2.8	8.6	5.4	9.4
Ga	4.2	6.0	1.95	−1.76	2.1	−3.41
In <sub>4</sub> Se <sub>3</sub>	15.8	−9.15	43.0	28.0	−7.24	2.76
PbBr <sub>2</sub>	−101	−111	51.6	55.9	11.1	25.6
LiGaO <sub>2</sub> , s <sup>E</sup>	0.55	2.35	−1.85	−1.15	2.35	1.25
MgBaF <sub>4</sub>	−3.95	−3.65	11.3	8.8	1.7	−1.1
Co <sub>2</sub> SiO <sub>4</sub>	−2.0	1.09	−2.46	−0.73	−0.95	−2.31
Rb <sub>2</sub> SO <sub>4</sub>	−2.85	−3.55	2.35	3.95	1.65	3.95

Table 1. Cont.

Crystals	$\Delta_1$ , TPa <sup>-1</sup>	$\Delta_2$ , TPa <sup>-1</sup>	$\Delta_3$ , TPa <sup>-1</sup>	$\Delta_4$ , TPa <sup>-1</sup>	$\Delta_5$ , TPa <sup>-1</sup>	$\Delta_6$ , TPa <sup>-1</sup>
AgTlSe	-4.85	11.0	87.6	143	104	143
NaNO <sub>2</sub>	-54.5	-74.2	-2.5	-23.8	-19.9	-21.5
$\alpha$ -S	40.0	52.0	26.5	-14.5	-18.0	-71.0
	-26.8	9.6	-35.3	-34.5	96.3	60.7
TbF <sub>3</sub>	1.55	-2.25	8.65	10.5	-3.72	1.9
Ni <sub>3</sub> B	4.37	3.73	2.77	1.6	3.63	3.1
$\alpha$ -U	-0.6	1.22	-1.97	-2.09	5.32	3.38
ZnSb	2.35	-0.05	7.65	7.25	-9.5	-7.5

Table 2. Values of Young's moduli  $E_1, E_2, E_3, E_4, E_5, E_6$  and  $E_7$  for some rhombic crystals. Global maximum and minimum values are shown in bold.

Crystals	$E_1$		$E_2$		$E_3$		$E_4$		$E_5$		$E_6$		$E_7$
	GP	Pa	GP										
Al <sub>2</sub> SiO <sub>5</sub>	<b>188</b>	Min	251	-	<b>310</b>	Max	247	Min	-	-	259	Max	-
CaSO <sub>4</sub>	90.9	Max	<b>175</b>	Max	105	-	90.5	-	71.6	-	<b>32.4</b>	Min	-
CaCO <sub>3</sub>	<b>144</b>	Max	75.8	Min	82.0	-	89.5	Max	<b>66.3</b>	Min	-	-	85.8
BaMnF <sub>4</sub> , s <sup>E</sup>	58.8	-	36.6	Min	<b>29.9</b>	Min	45.2	-	<b>90.1</b>	Max	-	-	-
BaSO <sub>4</sub>	58.1	Min	53.2	-	<b>92.6</b>	Max	<b>36.5</b>	Min	-	-	73.2	Max	-
Cs <sub>2</sub> SO <sub>4</sub>	32.7	Min	30.9	Min	<b>27.5</b>	Min	32.9	-	33.4	-	<b>33.7</b>	Max	-
BeAl <sub>2</sub> O <sub>4</sub>	<b>478</b>	Max	386	Max	417	-	<b>372</b>	Min	374	-	379	-	-
MgSiO <sub>3</sub>	190	-	<b>148</b>	Min	192	-	-	-	182	Min	<b>202</b>	Max	-
Mg <sub>2</sub> SiO <sub>4</sub>	<b>297</b>	Max	171	-	203	-	<b>171</b>	Min	199	-	-	-	-
Ga	82.0	Min	<b>71.4</b>	Min	<b>118</b>	Max	-	-	-	-	95.5	Max	-
In <sub>4</sub> Se <sub>3</sub>	<b>23.8</b>	Min	58.8	Max	37.0	-	-	-	<b>62.7</b>	Max	-	-	-
I	<b>3.05</b>	Min	9.71	-	7.58	-	6.24	Min	<b>30.8</b>	Max	13.5	Max	-
La <sub>2</sub> CuO <sub>4</sub>	117	Min	<b>116</b>	Min	159	-	161	-	161	-	<b>202</b>	Max	-
PbBr <sub>2</sub>	19.7	-	24.7	-	18.2	-	27.0	Max	<b>38.7</b>	Max	<b>10.1</b>	Min	-
LiGaO <sub>2</sub> , s <sup>E</sup>	137	-	<b>110</b>	Min	125	-	132	Max	118	Min	<b>139</b>	Max	130
MgBaF <sub>4</sub>	70.9	-	69.4	-	86.2	-	-	-	<b>129</b>	Max	<b>61.9</b>	Min	72.8
C <sub>6</sub> N <sub>2</sub> O <sub>3</sub> H <sub>6</sub>	7.0	-	4.91	Min	<b>3.51</b>	Min	<b>19.6</b>	Max	-	-	13.7	-	-
Co <sub>2</sub> SiO <sub>4</sub>	<b>240</b>	Max	138	-	170	-	<b>133</b>	Min	165	-	-	-	-
Mg <sub>2</sub> GeO <sub>4</sub>	<b>282</b>	Max	161	-	187	-	<b>153</b>	Min	173	-	-	-	-
Ni <sub>2</sub> SiO <sub>4</sub>	<b>270</b>	Max	<b>175</b>	Min	189	-	192	-	-	-	-	-	-
KNO <sub>3</sub>	<b>26.4</b>	Max	20.1	-	15.4	-	-	-	<b>14.4</b>	Min	-	-	19.2
K <sub>2</sub> SeO <sub>4</sub>	<b>40.3</b>	Max	39.5	Max	30.6	-	<b>24.7</b>	Min	-	-	37.6	-	-
K <sub>2</sub> SO <sub>4</sub>	42.4	-	45.9	-	44.2	-	<b>47.4</b>	Max	46.7	Max	<b>38.4</b>	Min	-
K <sub>2</sub> ZnCl <sub>4</sub>	15.6	Max	15.7	Max	<b>20.8</b>	Max	15.2	-	14.8	-	<b>13.3</b>	Min	-
RbHSO <sub>4</sub>	22.9	-	30.1	-	<b>32.6</b>	Max	<b>14.3</b>	Min	15.7	Min	31.5	Max	-
Rb <sub>2</sub> SO <sub>4</sub>	38.8	-	39.8	-	<b>36.5</b>	Min	<b>40.6</b>	Max	40.1	Max	36.9	Min	-
Rb <sub>2</sub> ZnBr <sub>4</sub>	12.2	-	12.9	Max	<b>16.9</b>	Max	12.5	-	-	-	<b>10.0</b>	Min	-
Al <sub>2</sub> SiO <sub>5</sub>	242	Max	<b>153</b>	Min	279	-	<b>325</b>	Max	196	Min	-	-	225
AgNO <sub>3</sub>	<b>11.3</b>	Min	13.5	Min	<b>29.2</b>	Max	-	-	-	-	25.6	Max	-
AgTlSe	18.7	-	14.4	Min	<b>9.17</b>	Min	38.8	-	<b>49.6</b>	Max	-	-	-
NaBF <sub>4</sub>	39.4	Max	29.9	-	<b>51.7</b>	Max	-	-	<b>13.9</b>	Min	29.6	-	-
Na <sub>2</sub> GeO <sub>3</sub> , s <sup>E</sup>	66.0	-	83.8	Max	71.4	-	-	-	<b>94.7</b>	Max	<b>54.5</b>	Min	-
NaNO <sub>2</sub>	25.1	Max	49.8	Max	<b>54.1</b>	Max	33.7	-	25.0	-	<b>15.9</b>	Min	-
Na <sub>2</sub> SO <sub>4</sub>	65.4	Max	<b>93.5</b>	Max	58.8	-	<b>42.6</b>	Min	51.1	-	63.0	-	-
SrSO <sub>4</sub>	45.5	Min	45.9	-	<b>87.7</b>	Max	<b>39.0</b>	Min	-	-	74.6	Max	-
$\alpha$ -S	14.1	Min	12.0	-	<b>33.3</b>	Max	<b>11.5</b>	Min	-	-	18.7	Max	-
	13.4	Max	<b>9.01</b>	Min	13.3	-	<b>19.3</b>	Max	10.8	Min	-	-	11.6
Mn <sub>2</sub> SiO <sub>4</sub>	<b>198</b>	Max	<b>116</b>	Min	146	-	-	-	143	-	-	-	-
TbF <sub>3</sub>	101	Min	163	Max	<b>85.1</b>	Min	-	-	<b>166</b>	Max	-	-	-
Tl <sub>2</sub> SO <sub>4</sub>	21.7	Min	<b>21.0</b>	Min	27.7	-	<b>28.2</b>	Max	27.9	-	22.2	-	-
Ni <sub>3</sub> B	<b>150</b>	Min	166	Min	182	-	<b>246</b>	Max	203	-	232	-	-
$\alpha$ -U	204	Max	<b>149</b>	Min	209	-	<b>288</b>	Max	170	Min	-	-	189
ZnSb	72.5	Min	87.7	Max	74.6	-	<b>59.8</b>	Min	<b>101</b>	Max	-	-	81.7

**Table 3.** The values of the minimum and maximum Young's moduli  $E_{\min}$ ,  $E_{\max}$  and their ratios,  $E_{\max}/E_{\min}$ ; and the values of the minimum and maximum Poisson's ratios,  $\nu_{\min}$  and  $\nu_{\max}$ .

Crystals	$E_{\min}$	$E_{\max}$	$E_{\max}/E_{\min}$	$\nu_{\min}$	$\nu_{\max}$
$(\text{CH}_3)_3\text{NCH}_2\text{COO}\cdot(\text{CH}_2)(\text{COOH})_2$	2.92	37.0	12.7	−0.05	0.91
I	3.05	30.8	10.1	−0.48	1.31
$\text{SC}(\text{NH}_2)_2$	2.39	23.8	9.96	−0.28	1.00
	2.09	24.6	11.8	−0.37	1.07
$(\text{CH}_3)_3\text{NCH}_2\text{COO}\cdot\text{H}_3\text{BO}_3$	1.85	18.3	9.89	−0.39	1.22
Cu-14 wt% Al 3.0 wt% Ni	22.3	167	7.49	−0.70	1.43
$\text{NH}_4\text{B}_5\text{O}_8\cdot 4\text{H}_2\text{O}$	6.85	50.7	7.40	−0.10	0.85
$\text{NH}_4\text{HC}_2\text{O}_4\cdot 1/2\text{H}_2\text{O}$	10.5	61.0	5.81	0.05	0.82
$\text{C}_6\text{N}_2\text{O}_3\text{H}_6$	3.51	19.6	5.58	−0.91	1.05
$(\text{Fe,Mg})_2(\text{Al,Fe}^{+3})_9\text{O}_6\text{SiO}_4(\text{O,OH})_2$	57.8	312	5.40	−0.20	0.95
$\text{CaSO}_4$	32.4	175	5.40	−0.05	0.76
$\text{AgTlSe}$	9.17	49.5	5.40	−0.42	1.07
$\text{CH}_3\text{COOLi}\cdot 2\text{H}_2\text{O}$	11.6	53.8	4.64	0.04	0.68
$\text{CaPb}(\text{CN})_4\cdot 5\text{H}_2\text{O}$	9.79	43.5	4.44	0.07	0.71
$(\text{CD})_4\text{N}_2$	4.46	19.2	4.30	0.00	0.71
$\text{KB}_5\text{O}_8\cdot 4\text{H}_2\text{O}$	10.2	43.1	4.22	0.06	0.82
$\text{Cd}(\text{COOH})_2$	8.06	33.3	4.13	−0.09	0.98
$\text{C}_{24}\text{H}_{18}$	3.22	13.1	4.07	−0.06	0.77
$\text{Ca}(\text{COOH})_2$	11.8	47.8	4.05	−0.23	0.81
$\text{C}_{14}\text{H}_{12}\text{N}_2$	2.84	11.0	3.87	−0.02	0.76
$\text{PbBr}_2$	10.1	38.7	3.83	−0.19	0.90
$\text{NaBF}_4$	13.9	51.7	3.72	−0.05	0.71
$(\text{CH}_3\text{NHCH}_2\text{COOH})_3\cdot \text{CaCl}_2$	12.6	44.9	3.56	−0.48	0.76
$\text{Na}_2\text{C}_4\text{H}_4\text{O}_6\cdot 2\text{H}_2\text{O}$	11.0	37.9	3.45	−0.05	0.88
$\text{C}_6\text{H}_4(\text{NO}_2)_2$	5.68	19.4	3.42	−0.01	0.60
NIPC	2.39	8.15	3.41	−0.16	0.84
$\text{NaNO}_2$	15.9	54.1	3.40	0.09	0.64
$\text{CsSCN}$	6.38	21.1	3.31	0.01	0.78
$(\text{CH}_3)_3\text{NCH}_2\text{COO}\cdot \text{CaCl}_2\cdot 2\text{H}_2\text{O}$	7.63	23.6	3.09	−0.08	0.79
$\text{C}_6\text{H}_8\text{O}_7\text{H}_2\text{O}$	8.61	26.4	3.07	0.00	0.74
$\text{C}_5\text{H}_{10}\text{ClNO}_4$	9.90	30.3	3.06	0.05	0.61
$\text{ZnSO}_4\cdot 7\text{H}_2\text{O}$	16.1	48.8	3.03	−0.15	0.71
	15.6	30.0	1.92	−0.04	0.66
$[\text{CN}_3\text{H}_6]_2\text{C}_8\text{H}_4\text{O}_4$	3.61	10.9	3.02	−0.28	0.94
$\text{BaMnF}_4, s^E$	29.9	90.1	3.01	−0.05	0.87

## 2. Young's Modulus

This expression for the reciprocal of Young's modulus is obtained as the ratio of the tensile force uniformly distributed over the transverse surface to the relative elongation using Hooke's law for an anisotropic material. Young's modulus  $E(\mathbf{n})$  for anisotropic materials depends on the tensor compliance coefficients  $s_{ijkl}$  and direction of the axis of extension [104]:

$$\frac{1}{E(\mathbf{n})} = s_{ijkl}n_i n_j n_k n_l.$$

Here  $n_i$  are the components of the unit vector  $\mathbf{n}$ , which is directed along the axis of extension. Rhombic crystals are characterized by nine independent matrix compliance coefficients  $s_{11}$ ,  $s_{22}$ ,  $s_{33}$ ,  $s_{44}$ ,  $s_{55}$ ,  $s_{66}$ ,  $s_{12}$ ,  $s_{13}$  and  $s_{23}$  [105]. The matrix of compliance coefficients is represented as follows

$$\begin{pmatrix} s_{11} & s_{12} & s_{13} & 0 & 0 & 0 \\ s_{12} & s_{22} & s_{23} & 0 & 0 & 0 \\ s_{13} & s_{23} & s_{33} & 0 & 0 & 0 \\ 0 & 0 & 0 & s_{44} & 0 & 0 \\ 0 & 0 & 0 & 0 & s_{55} & 0 \\ 0 & 0 & 0 & 0 & 0 & s_{66} \end{pmatrix}.$$

Using the matrix compliance coefficients, the expression for Young's modulus of rhombic crystals can be written as

$$E^{-1}(\mathbf{n}) = s_{11}n_1^4 + s_{22}n_2^4 + s_{33}n_3^4 + (2s_{23} + s_{44})n_2^2n_3^2 + (2s_{13} + s_{55})n_1^2n_3^2 + (2s_{12} + s_{66})n_1^2n_2^2. \quad (1)$$

If the orientation of the crystalline rod in the crystallographic coordinate system is described with three Euler's angles  $\varphi, \theta, \psi$ , then using the relationship between the unit vector  $\mathbf{n}$  and Euler's angles  $\varphi, \theta$ ,

$$\mathbf{n} = \begin{pmatrix} \sin \varphi \sin \theta \\ -\cos \varphi \sin \theta \\ \cos \theta \end{pmatrix},$$

the expression of Young's modulus  $E$  for rhombic crystals can be rewritten as follows.

$$E^{-1}(\varphi, \theta) = [s_{11} \sin^4 \varphi + s_{22} \cos^4 \varphi + 0.25(2s_{12} + s_{66}) \sin^2 2\varphi] \sin^4 \theta + s_{33} \cos^4 \theta + 0.25[(2s_{23} + s_{44}) \cos^2 \varphi + (2s_{13} + s_{55}) \sin^2 \varphi] \sin^2 2\theta \quad (2)$$

The dependence of Young's modulus for rhombic crystals is a periodic function  $\varphi$  and  $\theta$  with periods  $T_\varphi = \pi$  and  $T_\theta = \pi$ .

It is convenient to introduce six anisotropy coefficients of rhombic crystals for analyzing the variability of Young's modulus:

$$\begin{aligned} \Delta_1 &\equiv s_{11} - s_{12} - 0.5s_{66}, & \Delta_2 &\equiv s_{22} - s_{12} - 0.5s_{66}, \\ \Delta_3 &\equiv s_{11} - s_{13} - 0.5s_{55}, & \Delta_4 &\equiv s_{33} - s_{13} - 0.5s_{55}, \\ \Delta_5 &\equiv s_{22} - s_{23} - 0.5s_{44}, & \Delta_6 &\equiv s_{33} - s_{23} - 0.5s_{44}, \end{aligned} \quad (3)$$

which disappear in the limit of an isotropic medium. The number of anisotropy coefficients of rhombic crystals is greater than those of the cubic, hexagonal and tetragonal crystals. The last crystals have one [105,106], two [8,12] and three [9] anisotropy coefficients, respectively. The values of the anisotropy coefficients for some rhombic crystals are given in Table 1, and in Table S1 from the Supplementary Material the values for all rhombic crystals from the reference book [4] are presented.

### 3. Stationary and Extreme Values of Young's Modulus

The necessary conditions for extremum of Young's modulus are the stationarity conditions

$$\frac{\partial E(\varphi, \theta)}{\partial \varphi} = 0, \quad \frac{\partial E(\varphi, \theta)}{\partial \theta} = 0. \quad (4)$$

These conditions using (2) lead to a system of equations:

$$\begin{cases} [((\Delta_1 + \Delta_2) \sin^2 \varphi - \Delta_2) \sin^2 \theta + \Delta_0 \cos^2 \theta] \sin^2 \theta \sin 2\varphi = 0 \\ \left[ (s_{11} \sin^4 \varphi + s_{22} \cos^4 \varphi + 0.25(2s_{12} + s_{66}) \sin^2 2\varphi - (s_{13} + 0.5s_{55}) \sin^2 \varphi - (s_{23} + 0.5s_{44}) \cos^2 \varphi) \sin^2 \theta + \right. \\ \left. + ((s_{13} + 0.5s_{55}) \sin^2 \varphi + (s_{23} + 0.5s_{44}) \cos^2 \varphi - s_{33}) \cos^2 \theta \right] \sin 2\theta = 0 \end{cases} \quad (5)$$

Here  $\Delta_0 = \Delta_6 - \Delta_4 = \Delta_5 - \Delta_3 = s_{13} - s_{23} + 0.5s_{55} - 0.5s_{44}$ . Four solutions to the first equation are  $\theta = 0$ ;  $\varphi = 0$ ;  $\varphi = \pi/2$ ;  $\tan^2 \theta = -\Delta_0 / ((\Delta_1 + \Delta_2) \sin^2 \varphi - \Delta_2)$ . By substituting them into the second equation of system (5), one can find seven stationary values of Young's modulus.

At  $\varphi = \pi/2$  and  $\theta = \pi/2$  stationary value

$$E_1 = E_{[100]} = \frac{1}{s_{11}} \quad (6)$$

is achieved. It corresponds to stretching in the [100] direction.

The second stationary value of Young's modulus

$$E_2 = E_{[010]} = \frac{1}{s_{22}} = \frac{1}{s_{11} + \Delta_2 - \Delta_1} \quad (7)$$

is achieved at  $\varphi = 0, \theta = \pi/2$  and  $\varphi = \pi, \theta = \pi/2$ . It corresponds to stretching in the  $[0\bar{1}0]$  and  $[010]$  directions.

The third value also has a simple form,

$$E_3 = E_{[001]} = \frac{1}{s_{33}} = \frac{1}{s_{11} + \Delta_4 - \Delta_3}, \quad (8)$$

and is achieved at  $\theta = 0$  and an arbitrary angle  $\varphi$ . This stationary value corresponds to stretching in the  $[001]$  direction.

At  $\varphi = 0$  the fourth stationary value of Young's modulus has the form

$$E_4 = \frac{E_2 E_3 (\Delta_5 + \Delta_6)^2}{E_2 \Delta_5^2 + E_3 \Delta_6^2 + 2E_3 (1 - \Delta_5 E_2) \Delta_5 \Delta_6} \quad (9)$$

at the limitations

$$\tan^2 \theta = \frac{\Delta_6}{\Delta_5} \geq 0. \quad (10)$$

This value corresponds to stretching in the  $(100)$  plane. Young's moduli  $E_2$  and  $E_3$  also lie in the  $(100)$  plane.

At  $\varphi = \pi/2$  the fifth stationary value of Young's modulus has the form

$$E_5 = \frac{E_1 E_3 (\Delta_3 + \Delta_4)^2}{E_1 \Delta_3^2 + E_3 \Delta_4^2 + 2E_3 (1 - \Delta_3 E_1) \Delta_3 \Delta_4} \quad (11)$$

with the limitations

$$\tan^2 \theta = \frac{\Delta_4}{\Delta_3} \geq 0. \quad (12)$$

This value corresponds to stretching in the  $(010)$  plane. Young's moduli  $E_1$  and  $E_3$  also lie in the  $(010)$  plane.

At  $\theta = \pi/2$  the sixth stationary value of Young's modulus has the form

$$E_6 = \frac{E_1 E_2 (\Delta_1 + \Delta_2)^2}{E_1 \Delta_1^2 + E_2 \Delta_2^2 + 2E_2 (1 - \Delta_1 E_1) \Delta_1 \Delta_2} \quad (13)$$

with the limitation

$$\tan^2 \varphi = \frac{\Delta_2}{\Delta_1} \geq 0. \quad (14)$$

This value corresponds to stretching in the  $(001)$  plane. Young's moduli  $E_1$  and  $E_2$  also lie in the  $(001)$  plane.

The seventh stationary value of Young's modulus has the form (2) with the constraints

$$\tan^2 \theta = -\frac{\Delta_0}{(\Delta_1 + \Delta_2) \sin^2 \varphi - \Delta_2} \geq 0, \quad (15)$$

$$0 \leq \sin^2 \varphi = \frac{\Delta_0 \Delta_5 - \Delta_2 \Delta_6}{\Delta_0^2 + \Delta_0 \Delta_2 - \Delta_6 (\Delta_1 + \Delta_2)} \leq 1. \quad (16)$$

We further investigate these stationary points using the sufficient condition for the extremum of the function of two variables. If at the indicated stationary points from the second derivatives of Young's modulus,

$$A = \frac{\partial^2 E}{\partial \varphi^2}, \quad B = \frac{\partial^2 E}{\partial \varphi \partial \theta}, \quad C = \frac{\partial^2 E}{\partial \theta^2}, \quad (17)$$

a combination is formed

$$D = AC - B^2,$$

then at  $D > 0$  extremes of Young's modulus are achieved at the corresponding stationary point (maximum at  $A < 0$  and  $C < 0$  or minimum at  $A > 0$  and  $C > 0$ ). In the case  $D < 0$ , extrema are absent at the stationary point, and at  $D = 0$  additional analysis is required [107].

In the case of a stationary point  $\varphi = \pi/2, \theta = \pi/2$ , we have  $E = E_1$  and

$$D = \frac{16\Delta_1\Delta_2}{s_{11}^4}, \quad A = \frac{4\Delta_1}{s_{11}^2}, \quad C = \frac{4\Delta_2}{s_{11}^2}, \quad B = 0.$$

Then, according to the sufficient condition for the extremum of the function, the value of Young's modulus  $E_1$  will be extremal if  $\Delta_1\Delta_3 > 0$ . The value  $E_1$  will be the maximum at  $\Delta_1 < 0$  or  $\Delta_3 < 0$  and the minimum at  $\Delta_1 > 0$  or  $\Delta_3 > 0$ .

In the case of a stationary points  $\varphi = 0, \theta = \pi/2$  and  $\varphi = \pi, \theta = \pi/2$ , we have  $E = E_2$  and

$$D = \frac{16\Delta_2\Delta_5}{s_{22}^4}, \quad A = \frac{4\Delta_2}{s_{22}^2}, \quad C = \frac{4\Delta_5}{s_{22}^2}, \quad B = 0.$$

The value of Young's modulus  $E_2$  will be extreme if  $\Delta_2\Delta_5 > 0$ . The value  $E_2$  is the maximum at  $\Delta_2 < 0$  or  $\Delta_5 < 0$  and minimum at  $\Delta_2 > 0$  or  $\Delta_5 > 0$ .

At  $\theta = 0$  and an arbitrary angle  $\varphi$  we have  $E = E_3$  and combination of coefficients  $D$  vanishes. As a result, additional analysis is required for each specific crystal. The value  $E_3$  will be the extremum of 44 (from 142) rhombic crystals. For example, such crystals are Ga ( $E_3 = E_{\max}$ ),  $\text{NH}_4\text{ClO}_4$  ( $E_3 = E_{\max}$ ),  $\text{Al}_2\text{SiO}_5$  ( $E_3 = E_{\max}$ ),  $\text{BaSO}_4$  ( $E_3 = E_{\max}$ ),  $\text{Cs}_2\text{SO}_4$  ( $E_3 = E_{\min}$ ) and  $\text{LiCsSO}_4$  ( $E_3 = E_{\min}$ ),  $\text{AgTlSe}$  ( $E_3 = E_{\min}$ ),  $\text{TbF}_3$  ( $E_3 = E_{\min}$ ) (see Table 2 and Table S2 in the Supplementary Material).

For the stationary values of Young's modulus— $E_4, E_5, E_6$  and  $E_7$ —the second derivatives  $A, B, C$  and  $D$  have a cumbersome analytical form. Therefore, only numerical analysis of them for 142 rhombic crystals was carried out. The results of this analysis are presented in Table 2 and Table S2 in the Supplementary Material. In Table S2 in the Supplementary Material for the values of Young's modulus  $E_4, E_5, E_6$  and  $E_7$ , the values of the angles at which they are achieved are also given. In these tables, the global maximum and minimum values of Young's modulus are shown in bold. An analysis of the variability of Young's modulus showed that the value  $E_7$  is the inflection point for all rhombic crystals from [4].

The largest differences between the maximum and minimum values of Young's modulus were found in  $(\text{CH}_3)_3\text{NCH}_2\text{COO}\cdot(\text{CH}_2)(\text{COOH})_2$  ( $E_{\max}/E_{\min} = 12.7$ ), I ( $E_{\max}/E_{\min} = 10.1$ ) and  $\text{SC}(\text{NH}_2)_2$  ( $E_{\max}/E_{\min} = 9.96$ ; for the second set of elastic constants  $E_{\max}/E_{\min} = 11.8$ ),  $(\text{CH}_3)_3\text{NCH}_2\text{COO}\cdot\text{H}_3\text{BO}_3$  ( $E_{\max}/E_{\min} = 9.92$ ), Cu-14 wt% Al, 3.0 wt% Ni ( $E_{\max}/E_{\min} = 7.51$ ),  $\text{NH}_4\text{B}_5\text{O}_8\cdot 4\text{H}_2\text{O}$  ( $E_{\max}/E_{\min} = 7.39$ ),  $\text{NH}_4\text{HC}_2\text{O}_4\cdot 1/2\text{H}_2\text{O}$  ( $E_{\max}/E_{\min} = 5.83$ ),  $\text{C}_6\text{N}_2\text{O}_3\text{H}_6$  ( $E_{\max}/E_{\min} = 5.58$ ),  $\text{CaSO}_4$  ( $E_{\max}/E_{\min} = 5.4$ ). The maximum Young's modulus was revealed in  $\text{BeAl}_2\text{O}_4$  ( $E_{\max} = 478$  GPa). Thus, among rhombic crystals, no materials were found for which  $E_{\max} > 500$  GPa, in contrast to materials with tetragonal, hexagonal and cubic anisotropy (see Section 4).

Among rhombic crystals, more than 50 auxetics (materials with negative Poisson's ratios) were detected. The smallest values of Poisson's ratio were for  $\text{C}_6\text{N}_2\text{O}_3\text{H}_6$  ( $\nu_{\min} = -0.91$ ), Cu-14wt %Al, 3.0wt %Ni ( $\nu_{\min} = -0.70$ ), I ( $\nu_{\min} = -0.48$ ),  $(\text{CH}_3\text{NHCH}_2\text{COOH})_3\cdot\text{CaCl}_2$  ( $\nu_{\min} = -0.48$ ),  $\text{AgTlSe}$  ( $\nu_{\min} = -0.42$ ),  $(\text{CH}_3)_3\text{NCH}_2\text{COO}\cdot\text{H}_3\text{BO}_3$  ( $\nu_{\min} = -0.39$ ),  $\text{Sr}(\text{COOH})_2\cdot 2\text{H}_2\text{O}$  ( $\nu_{\min} = -0.39$ ),  $\text{SC}(\text{NH}_2)_2$  ( $\nu_{\min} = -0.37$ ). As can be seen, most materials that have a maximum value of ratio  $E_{\max}/E_{\min}$  have the smallest values of Poisson's ratio. The data from Table 3 and Table S3 from the Supplementary Material confirm this. Thirty-three rhombic crystals with  $E_{\max}/E_{\min} > 3$  are shown in Table 3. Twenty-four

crystals of them have negative Poisson's ratios. The remaining ten crystals from this table have small positive values for the minimum Poisson's ratio. These values range from 0 to 0.1. The values  $E_{\max}/E_{\min}$  and extremum values of Poisson's ratio for all rhombic crystals from [4] are given in Table S3 from the Supplementary Material.

In Figure 1, the classification scheme for three stationary values of Young's modulus  $E_1, E_2$  and  $E_3$  depending on two dimensionless parameters is presented,  $\alpha = (\Delta_2 - \Delta_1)/s_{11}$  and  $\beta = (\Delta_4 - \Delta_3)/s_{11}$ . The points indicate the values of dimensionless parameters  $\alpha$  and  $\beta$  for 142 rhombic crystals from [4]. Most crystals fall into the area  $-1 < \alpha < 1$  and  $-1 < \beta < 1$ . There are six zones on the classification scheme, in which various inequalities between the stationary values of Young's modulus  $E_1, E_2, E_3$  are satisfied. For each of these zones, the surface of Young's moduli for some rhombic crystals are shown in Figure 2.

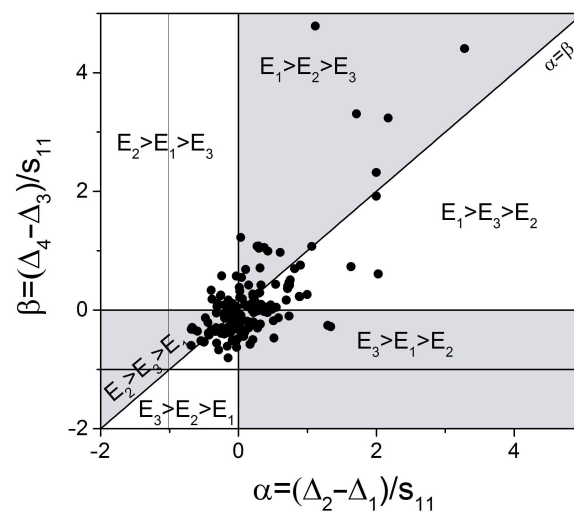


**Figure 1.** Classification scheme for stationary values of Young's modulus ( $E_1, E_2$  and  $E_3$ ) for rhombic crystals. The points indicate the values of dimensionless parameters  $\alpha$  and  $\beta$  for 142 rhombic crystals from [4].

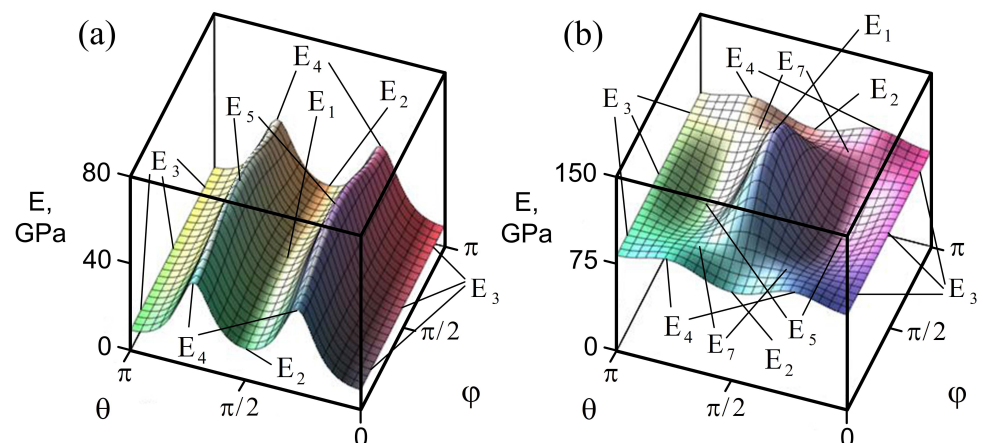


**Figure 2.** Cont.

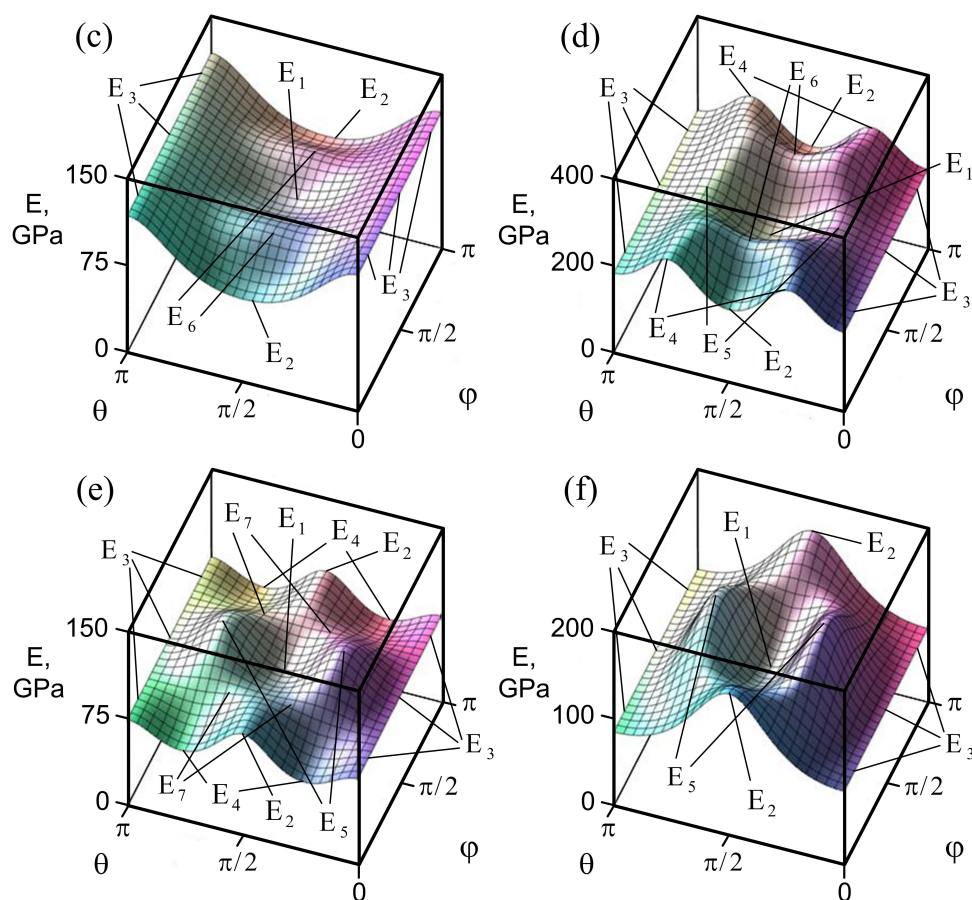


**Figure 2.** Young's modulus surfaces for rhombic crystals related to one of six zones: AgTlSe ( $E_1 > E_2 > E_3$ ) (a), CaCO<sub>3</sub> ( $E_1 > E_3 > E_2$ ) (b), Ga ( $E_3 > E_1 > E_2$ ) (c), Ni<sub>3</sub>B ( $E_3 > E_2 > E_1$ ) (d), ZnSb ( $E_2 > E_3 > E_1$ ) (e) or TbF<sub>3</sub> ( $E_2 > E_1 > E_3$ ) (f).

#### 4. Young's Moduli of Tetragonal, Hexagonal and Cubic Crystals

Above, the stationary values of Young's modulus for rhombic crystals were shown. Below we present the stationary values of Young's modulus for tetragonal, hexagonal and cubic crystals as special cases of rhombic crystals. Rhombic crystals are characterized by nine independent compliance coefficients  $s_{11}, s_{22}, s_{33}, s_{44}, s_{55}, s_{66}, s_{12}, s_{13}$  and  $s_{23}$ , and six anisotropy coefficients (see Formulas (3)).

##### 4.1. Tetragonal Crystals

Tetragonal crystals have six independent compliance coefficients, which are obtained under three conditions,  $s_{11} = s_{22}, s_{44} = s_{55}$  and  $s_{13} = s_{23}$ , for nine compliance coefficients that were given previously.

The expression of Young's modulus for six-constant tetragonal crystals takes the form

$$E^{-1}(\varphi, \theta) = (s_{11} - 0.5\Delta_1 \sin^2 2\varphi) \sin^4 \theta + s_{33} \cos^4 \theta + 0.25(2s_{13} + s_{44}) \sin^2 2\theta.$$

The dependence of Young's modulus for six-constant tetragonal crystals is a periodic function  $\varphi, \theta$  with periods  $T_\varphi = \pi/2$  and  $T_\theta = \pi$ . Such crystals will already have three anisotropy coefficients,

$$\Delta_1 \equiv s_{11} - s_{12} - 0.5s_{66}, \quad \Delta_2 \equiv s_{11} - s_{12} - 0.5s_{44}, \quad \Delta_3 \equiv s_{33} - s_{13} - 0.5s_{44},$$

and five stationary values of Young's modulus.

1. At  $\varphi = \pi/2, \theta = \pi/2, \varphi = 0, \theta = \pi/2$  the first stationary value has the form

$$E_1 = E_{[100]} = E_{[010]} = \frac{1}{s_{11}}$$

and is achieved by stretching in the [100] and [010] directions.

2. At  $\theta = 0$  and an arbitrary angle  $\varphi$  second stationary value

$$E_2 = E_{[001]} = \frac{1}{s_{33}}$$

takes place when stretched in the [001] direction.

3. At  $\varphi = \pi/4$ ,  $\theta = \pi/2$  the stationary value

$$E_3 = \frac{1}{s_{11} - 0.5\Delta_1}$$

is achieved by stretching in the (001) plane.

4. At  $\varphi = 0$ ,  $\varphi = \pi/2$  and limitation

$$\tan^2 \theta = \frac{\Delta_3}{\Delta_2} \geq 0$$

the fourth stationary value has the form

$$E_4 = \frac{E_1 E_2 (\Delta_2 + \Delta_3)^2}{E_1 \Delta_2^2 + E_2 \Delta_3^2 + 2E_1 (1 - \Delta_3 E_2) \Delta_2 \Delta_3}$$

This value corresponds to stretching in the (100) (at  $\varphi = 0$ ) and (010) (at  $\varphi = \pi/2$ ) planes. Young's moduli  $E_1$  and  $E_2$  also lie in the (100) and (010) planes.

5. In this case, the system of Equations (5) is greatly simplified, and it is possible to obtain a simple form for the fifth stationary value:

$$E_5 = \frac{E_2 E_3 (2\Delta_2 + 2\Delta_3 - \Delta_1)^2}{4E_2 \Delta_3^2 + E_3 (2\Delta_2 - \Delta_1)^2 + 4\Delta_3 E_3 (1 - \Delta_3 E_2) (2\Delta_2 - \Delta_1)}$$

which is achieved at  $\varphi = \pi/4$ ,  $\varphi = 3\pi/4$  and limitation

$$\tan^2 \theta = \frac{2\Delta_3}{2\Delta_2 - \Delta_1} \geq 0.$$

Young's moduli  $E_2$ ,  $E_3$  and  $E_5$  lie in the same plane.

A detailed analysis of the extreme values of Young's modulus for six-constant and seven-constant tetragonal crystals was carried out in [108].

The largest differences between the maximum and minimum values of Young's modulus were found in  $\text{Hg}_2\text{I}_2$  ( $E_{\max}/E_{\min} = 34.6$ ),  $\text{Hg}_2\text{Br}_2$  ( $E_{\max}/E_{\min} = 29.8$ ),  $\text{Hg}_2\text{Cl}_2$  ( $E_{\max}/E_{\min} = 24.0$ ),  $\text{TeO}_2$  ( $E_{\max}/E_{\min} = 12.6$ ; for the second set of elastic constants  $E_{\max}/E_{\min} = 14.2$ ) and  $(\text{NH}_2)_2\text{CO}$  ( $E_{\max}/E_{\min} = 11.6$ ; for the second set of elastic constants  $E_{\max}/E_{\min} = 24.1$ ). The maximum Young's modulus with  $E_{\max} > 500$  GPa was revealed in  $\text{PdPb}_2$  ( $E_{\max} = 684$  GPa), stishovite ( $E_{\max} = 654$  GPa). Among tetragonal crystals, 50 auxetics were found. Crystals with minimum Poisson's ratios of less than  $-0.5$  are  $\text{Hg}_2\text{Br}_2$  ( $\nu_{\min} = -1.02$ ),  $\text{Hg}_2\text{I}_2$  ( $\nu_{\min} = -0.96$ ),  $\text{Hg}_2\text{Cl}_2$  ( $\nu_{\min} = -0.91$ ) and  $(\text{NH}_2)_2\text{CO}$  ( $\nu_{\min} = -0.8$ ; for the second set of elastic constants  $\nu_{\min} = -0.98$ ),  $\text{TeO}_2$  ( $\nu_{\min} = -0.80$ ; for the second set of elastic constants  $\nu_{\min} = -0.85$ ) and  $\text{FeGe}_2$  ( $\nu_{\min} = -0.77$ ) [2,109]. Thus, tetragonal crystals with lowest Poisson's ratio have the greatest ratio  $E_{\max}/E_{\min}$ . Note that the minimum value of Poisson's ratio for  $\text{Hg}_2\text{Br}_2$  is less than  $-1$  (less than the lower boundary for isotropic materials).

#### 4.2. Hexagonal Crystals

Hexagonal crystals have five independent compliance coefficients, which are obtained under four conditions  $s_{11} = s_{22}$ ,  $s_{44} = s_{55}$ ,  $s_{13} = s_{23}$ ,  $s_{66} = 2(s_{11} - s_{12})$  for nine compliance coefficients of rhombic crystals previously given. The expression of Young's modulus for hexagonal crystals will take the form

$$E^{-1}(\theta) = s_{11} \sin^4 \theta + s_{33} \cos^4 \theta + 0.25(2s_{13} + s_{44}) \sin^2 2\theta.$$

Young's modulus of hexagonal crystals depends on only one Euler's angle  $\theta$ . The dependence of Young's modulus is a periodic function  $\theta$  with a period  $T_\theta = \pi$ . Hexagonal crystals already have two anisotropy coefficients:

$$\Delta_1 \equiv s_{11} - s_{12} - 0.5s_{44}, \quad \Delta_2 \equiv s_{33} - s_{13} - 0.5s_{44}$$

and three stationary values of Young's modulus.

1. At  $\theta = \pi/2$  the first stationary value has the form

$$E_1 = E_{(0001)} = \frac{1}{s_{11}}$$

and achieved by stretching in the (0001) plane.

2. At  $\theta = 0$  second stationary value

$$E_2 = E_{[0001]} = \frac{1}{s_{33}}$$

takes place in tension in the [0001] direction.

3. When limiting

$$\tan^2 \theta = \frac{\Delta_2}{\Delta_1} \geq 0$$

the third stationary value has the form

$$E_3 = \frac{E_1 E_2 (\Delta_1 + \Delta_2)^2}{E_1 \Delta_1^2 + E_2 \Delta_2^2 + 2E_1 (1 - \Delta_2 E_2) \Delta_1 \Delta_2}.$$

Young's moduli  $E_1$ ,  $E_2$  and  $E_3$  lie in the same plane.

A detailed analysis of the extreme values of Young's modulus and Poisson's ratio for hexagonal crystals was carried out in [12]. In this article, a classification scheme for the extreme values of Young's modulus  $E_1$ ,  $E_2$  and  $E_3$ , depending on two dimensionless parameters, is also given. The largest differences between the maximum and minimum values of Young's modulus were found in graphite ( $E_{\max}/E_{\min} = 71.8$ ), which has the greatest ratio among rhombic, tetragonal, hexagonal and cubic crystals. A large difference ( $E_{\max}/E_{\min} > 5$ ) was also revealed in  $\text{RbNiCl}_3$  ( $E_{\max}/E_{\min} = 5.52$ ) and  $\text{CsNiF}_3$  ( $E_{\max}/E_{\min} = 5.72$  for one experimental set of compliance coefficients and 10.6 for the second set of compliance coefficients) [12]. Maximum Young's modulus with  $E_{\max} > 500$  GPa were detected in graphite ( $E_{\max} = 1020$  GPa), WC ( $E_{\max} = 827$  GPa), SiC ( $E_{\max} = 556$  GPa), Re ( $E_{\max} = 588$  GPa) and Ru ( $E_{\max} = 550$  GPa). Graphite with hexagonal anisotropy and diamond with cubic anisotropy have the highest Young's moduli ( $E_{\max} > 1$  TPa) among the rhombic, tetragonal, hexagonal and cubic crystals from [4].

Among hexagonal crystals, six auxetics have been detected [12]. These crystals are  $\text{MoS}_2$  ( $\nu_{\min} = -0.28$ ),  $\text{C}_7\text{H}_{12}$  ( $\nu_{\min} = -0.15$ ), Zn ( $\nu_{\min} = -0.07$ ), MnAs ( $\nu_{\min} = -0.04$ ), Be-Cu at 2.4% ( $\nu_{\min} = -0.04$ ), Be ( $\nu_{\min} = -0.005$ ) and Be-Cu at 1.1% Cu ( $\nu_{\min} = -0.005$ ). This number of crystalline auxetics is the smallest among rhombic, tetragonal, hexagonal and cubic crystals. For hexagonal crystals, no relationship between the ratio  $E_{\max}/E_{\min}$  and negativity of Poisson's ratio was found, unlike rhombic, tetragonal and cubic crystals.

### 4.3. Cubic Crystals

Cubic crystals have only three independent compliance coefficients,  $s_{11} = s_{22} = s_{33}$ ,  $s_{44} = s_{55} = s_{66}$  and  $s_{12} = s_{13} = s_{23}$ . The expression of Young's modulus for cubic crystals has the form

$$E^{-1}(\varphi, \theta) = s_{11} - 0.5\Delta(\sin^2 2\theta + \sin^4 \theta \sin^2 2\varphi).$$

The dependence of Young's modulus is a periodic function  $\varphi, \theta$  with periods  $T_\varphi = \pi/2$  and  $T_\theta = \pi$ . Cubic crystals are characterized by one anisotropy coefficient

$$\Delta \equiv s_{11} - s_{12} - 0.5s_{44}$$

and have three stationary values of Young's modulus.

1. At  $\theta = 0$  and an arbitrary angle  $\varphi$ — $\varphi = \pi/2, \theta = \pi/2; \varphi = 0, \theta = \pi/2$ —the first stationary value has the form

$$E_1 = E_{[100]} = E_{[010]} = E_{[001]} = \frac{1}{s_{11}} \quad (18)$$

and is achieved by stretching in the [100], [010] and [001] directions.

2. At  $\varphi = 0, \theta = \pi/4; \varphi = \pi/2, \theta = \pi/4; \varphi = \pi/4, \theta = \pi/2$  the second stationary value

$$E_2 = E_{[110]} = \frac{1}{s_{11} - 0.5\Delta} = \frac{E_1}{1 - \Delta E_1/2} \quad (19)$$

is achieved by stretching in the [110] direction.

3. At  $\varphi = \pi/4, \tan \theta = \sqrt{2}$  the third stationary has the form

$$E_3 = E_{[111]} = \frac{1}{s_{11} - 2\Delta/3} = \frac{E_1}{1 - 2\Delta E_1/3} = \frac{E_2}{1 - \Delta E_2/6} \quad (20)$$

and corresponds to stretching in the [111] direction. This value is conveniently obtained from the fifth stationary value for tetragonal crystals.

Whether the magnitude of Young's modulus is the maximum or minimum depends on the sign and value of the anisotropy coefficient  $\Delta$ . For a subclass of cubic crystals with  $\Delta > 0$  from (18)–(20), inequalities follow:

$$E_{[111]} > E_{[110]} > E_{[100]}.$$

For example, Li, Na, K, Rb, Cs, Ca, Fe, Ni, Cu, Ag, Au, Al, C, Si and Ge have positive anisotropy coefficients ( $\Delta$ ).

For a subclass of cubic crystals with  $\Delta < 0$  from (18)–(20), opposite inequalities follow:

$$E_{[100]} > E_{[110]} > E_{[111]}.$$

For example, V, Cr, Mo and Nb have negative anisotropy coefficients ( $\Delta$ ).

The maximum Young's moduli with  $E_{\max} > 500$  GPa were detected in diamond ( $E_{\max} = 1207$  GPa), Ir ( $E_{\max} = 649$  GPa; for the second set of elastic constants  $E_{\max} = 620$  GPa),  $\text{ReO}_3$  ( $E_{\max} = 571$  GPa; for the second set of elastic constants  $E_{\max} = 478$  GPa),  $\text{NbC}_{0.865}$  ( $E_{\max} = 526$  GPa), SiC ( $E_{\max} = 511$  GPa; for the second set of elastic constants  $E_{\max} = 547$  GPa) and  $\text{CeB}_6$  ( $E_{\max} = 508$  GPa; for the second set of elastic constants  $E_{\max} = 472$  GPa). The largest differences between the maximum and minimum values of Young's modulus were found in InTl (25at%Tl) ( $E_{\max}/E_{\min} = 32.5$ ), InTl (28.13at%Tl) ( $E_{\max}/E_{\min} = 26.6$ ), InTl (27at%Tl) ( $E_{\max}/E_{\min} = 25.0$ ), InTl (30.16at%Tl) ( $E_{\max}/E_{\min} = 21.0$ ),  $\text{NiCr}_2\text{O}_4$  ( $E_{\max}/E_{\min} = 20.8$ ),  $\text{CuAuZn}_2$  ( $E_{\max}/E_{\min} = 15.8$ ),  $\text{Au}_{23}\text{Cu}_{30}\text{Zn}_{47}$  ( $E_{\max}/E_{\min} = 10.8$ ), InTl (39.06at%Tl) ( $E_{\max}/E_{\min} = 10.8$ ) and CuSi (4.17at%Si) ( $E_{\max}/E_{\min} = 10.2$ ). InTl alloys are shape memory materials. Additionally, a minimum value of Poisson's ratio of less than  $-1$  was detected in some InTl alloys [11,86,102]:  $\nu_{\min} = -1.17$  for InTl (25at%Tl) and  $\nu_{\min} = -1.02$  for InTl (27at%Tl). Some other crystals also have large negative Poisson's ratio values:  $\nu_{\min} = -0.81$

for InTl (28.13at%Tl),  $\nu_{\min} = -0.77$  for InTl (30.16at%Tl),  $\nu_{\min} = -0.59$  for InTl (39.06at%Tl),  $\nu_{\min} = -0.77$  for NiCr<sub>2</sub>O<sub>4</sub>,  $\nu_{\min} = -0.72$  for CuAuZn<sub>2</sub>,  $\nu_{\min} = -0.62$  for Au<sub>23</sub>Cu<sub>30</sub>Zn<sub>47</sub> and  $\nu_{\min} = -0.16$  for CuSi (4.17at%Si). In the case of cubic crystals, a relationship between the maximum ratio  $E_{\max}/E_{\min}$  and the negativity of Poisson's ratio can also be observed. All these crystals with negative Poisson's ratios have positive anisotropy ratios ( $\Delta$ ).

## 5. Conclusions

In the article, the variability of Young's moduli of rhombic crystals was analyzed. Analytical expressions of seven stationary values were obtained. Three stationary values always exist. Four other values occur when the additional conditions are met. In the case of rhombic crystals, the six stationary values of Young's modulus were revealed upon tension in the (100), (010) and (001) planes. Three of these values have a simple form and correspond to stretching in the [100], [010] and [001] directions. In addition, these six stationary values of Young's modulus can be extremes under certain conditions. The seventh stationary value is the inflection point for all 142 rhombic crystals indicated in [4].

Analytical stationary values of Young's modulus for tetragonal, hexagonal and cubic crystals were written out as special cases of rhombic crystals. Tetragonal crystals already have five stationary values of Young's modulus, whereas hexagonal and cubic crystals have three. In the case of tetragonal and hexagonal crystals, all stationary values can be global extrema under certain conditions. For cubic crystals, only two stationary values are global extrema ( $E_{[100]}$  or  $E_{[111]}$ ).

In the article, a numerical analysis of the stationary and extreme values of Young's modulus of rhombic crystals was also carried out, and the angles at which these values were revealed were determined. For three stationary values of Young's moduli of rhombic crystals corresponding to tension in the [100], [010] and [001] directions, a classification scheme based on two dimensionless parameters was presented. Rhombic crystals with strong anisotropy ( $E_{\max}/E_{\min}$ ) were detected.

More than 50 auxetics have been identified among rhombic crystals. The largest differences between the maximum and minimum values of Young's modulus of rhombic crystals were found in (CH<sub>3</sub>)<sub>3</sub>NCH<sub>2</sub>COO·(CH<sub>2</sub>)(COOH)<sub>2</sub> ( $E_{\max}/E_{\min} = 12.7$ ), I ( $E_{\max}/E_{\min} = 10.1$ ), SC(NH<sub>2</sub>)<sub>2</sub> ( $E_{\max}/E_{\min} = 9.96$ ; for the second set of elastic constants  $E_{\max}/E_{\min} = 11.8$ ), (CH<sub>3</sub>)<sub>3</sub>NCH<sub>2</sub>COO·H<sub>3</sub>BO<sub>3</sub> ( $E_{\max}/E_{\min} = 9.92$ ), Cu-14 wt%Al, 3.0wt%Ni ( $E_{\max}/E_{\min} = 7.51$ ), NH<sub>4</sub>B<sub>5</sub>O<sub>8</sub>·4H<sub>2</sub>O ( $E_{\max}/E_{\min} = 7.39$ ), NH<sub>4</sub>HC<sub>2</sub>O<sub>4</sub>·1/2H<sub>2</sub>O ( $E_{\max}/E_{\min} = 5.83$ ), C<sub>6</sub>N<sub>2</sub>O<sub>3</sub>H<sub>6</sub> ( $E_{\max}/E_{\min} = 5.58$ ) and CaSO<sub>4</sub> ( $E_{\max}/E_{\min} = 5.4$ ). Most of these crystals have negative minimum values of Poisson's ratio: (CH<sub>3</sub>)<sub>3</sub>NCH<sub>2</sub>COO·(CH<sub>2</sub>)(COOH)<sub>2</sub> ( $\nu_{\min} = -0.05$ ), I ( $\nu_{\min} = -0.48$ ), SC(NH<sub>2</sub>)<sub>2</sub> ( $\nu_{\min} = -0.37$ ), (CH<sub>3</sub>)<sub>3</sub>NCH<sub>2</sub>COO·H<sub>3</sub>BO<sub>3</sub> ( $\nu_{\min} = -0.39$ ), Cu-14wt%Al, 3.0wt%Ni ( $\nu_{\min} = -0.70$ ), NH<sub>4</sub>B<sub>5</sub>O<sub>8</sub>·4H<sub>2</sub>O ( $\nu_{\min} = -0.10$ ), C<sub>6</sub>N<sub>2</sub>O<sub>3</sub>H<sub>6</sub> ( $\nu_{\min} = -0.91$ ) and CaSO<sub>4</sub> ( $\nu_{\min} = -0.05$ ). Twenty-four of the thirty-three rhombic crystals with  $E_{\max}/E_{\min} > 3$  have negative Poisson's ratios.

The same relationship between these factors was revealed for crystals with tetragonal and cubic anisotropy. The largest differences between the maximum and minimum values of Young's modulus of tetragonal crystals were found in Hg<sub>2</sub>I<sub>2</sub> ( $E_{\max}/E_{\min} = 34.6$ ), Hg<sub>2</sub>Br<sub>2</sub> ( $E_{\max}/E_{\min} = 29.8$ ), Hg<sub>2</sub>Cl<sub>2</sub> ( $E_{\max}/E_{\min} = 24.0$ ), TeO<sub>2</sub> ( $E_{\max}/E_{\min} = 12.6$ ; for the second set of elastic constants  $E_{\max}/E_{\min} = 14.2$ ) and (NH<sub>2</sub>)<sub>2</sub>CO ( $E_{\max}/E_{\min} = 11.6$ ; for the second set of elastic constants  $E_{\max}/E_{\min} = 24.1$ ). All these crystals have negative minimum values of Poisson's ratio: Hg<sub>2</sub>I<sub>2</sub> ( $\nu_{\min} = -0.96$ ), Hg<sub>2</sub>Br<sub>2</sub> ( $\nu_{\min} = -1.02$ ), Hg<sub>2</sub>Cl<sub>2</sub> ( $\nu_{\min} = -0.91$ ), TeO<sub>2</sub> ( $\nu_{\min} = -0.80$ ; for the second set of elastic constants  $\nu_{\min} = -0.85$ ) and (NH<sub>2</sub>)<sub>2</sub>CO ( $\nu_{\min} = -0.8$ ; for the second set of elastic constants  $\nu_{\min} = -0.98$ ). In the case of cubic crystals, the largest differences between the maximum and minimum values of Young's modulus were found in InTl (25at%Tl) ( $E_{\max}/E_{\min} = 32.5$ ), InTl (28.13at%Tl) ( $E_{\max}/E_{\min} = 26.6$ ), InTl (27at%Tl) ( $E_{\max}/E_{\min} = 25.0$ ), InTl (30.16at%Tl) ( $E_{\max}/E_{\min} = 21.0$ ), NiCr<sub>2</sub>O<sub>4</sub> ( $E_{\max}/E_{\min} = 20.8$ ), CuAuZn<sub>2</sub> ( $E_{\max}/E_{\min} = 15.8$ ), Au<sub>23</sub>Cu<sub>30</sub>Zn<sub>47</sub> ( $E_{\max}/E_{\min} = 10.8$ ), InTl (39.06at%Tl) ( $E_{\max}/E_{\min} = 10.8$ ) and CuSi (4.17at%Si) ( $E_{\max}/E_{\min} = 10.2$ ). All these crystals have negative minimum values of Pois-

son's ratio: InTl (25at%Tl) ( $\nu_{\min} = -1.17$ ), InTl (28.13at%Tl) ( $\nu_{\min} = -0.81$ ), InTl (27at%Tl) ( $\nu_{\min} = -1.02$ ), InTl (30.16at%Tl) ( $\nu_{\min} = -0.77$ ), NiCr<sub>2</sub>O<sub>4</sub> ( $\nu_{\min} = -0.77$ ), CuAuZn<sub>2</sub> ( $\nu_{\min} = -0.72$ ), Au<sub>23</sub>Cu<sub>30</sub>Zn<sub>47</sub> ( $\nu_{\min} = -0.62$ ), InTl (39.06at%Tl) ( $\nu_{\min} = -0.59$ ) and CuSi (4.17at%Si) ( $\nu_{\min} = -0.16$ ). For hexagonal crystals, the relationship between the largest ratio  $E_{\max}/E_{\min}$  and the minimum value of Poisson's ratio was not revealed.

**Supplementary Materials:** The following are available online at <https://www.mdpi.com/article/10.3390/cryst11080863/s1>. Table S1: Values of anisotropy coefficients  $\Delta_1, \Delta_2, \Delta_3, \Delta_4, \Delta_5$  and  $\Delta_6$  of rhombic crystals. Table S2: Values of Young's modulus,  $E_1, E_2, E_3, E_4, E_5, E_6$  and  $E_7$ , for rhombic crystals. Global maximum and minimum values are shown in bold. Angle values are given in degrees. Table S3: The values of the minimum and maximum Young's moduli  $E_{\min}$  and  $E_{\max}$  and their ratios  $E_{\max}/E_{\min}$ ; and the values of the minimum and maximum Poisson's ratios  $\nu_{\min}$  and  $\nu_{\max}$ .

**Author Contributions:** Conceptualization, methodology, V.A.G. and D.S.L.; software, formal analysis, D.S.L.; writing—original draft preparation, D.S.L. Both authors have read and agreed to the published version of the manuscript.

**Funding:** The reported study was funded by the Government program of IPMech RAS AAAA-A20-120011690136-2 and by RFBR, project number 20-31-70035.

**Institutional Review Board Statement:** Not applicable.

**Informed Consent Statement:** Not applicable.

**Data Availability Statement:** Data sharing not applicable.

**Conflicts of Interest:** The authors declare no conflict of interest.

## References

1. Ting, T.C.T.; Chen, T. Poisson's ratio for anisotropic elastic materials can have no bounds. *Quart. J. Mech. Appl. Math.* **2005**, *58*, 73–82. [[CrossRef](#)]
2. Lethbridge, Z.A.D.; Walton, R.I.; Marmier, A.S.H.; Smith, C.W.; Evans, K.E. Elastic anisotropy and extreme Poisson's ratios in single crystals. *Acta Mater.* **2010**, *58*, 6444–6451. [[CrossRef](#)]
3. Goldstein, R.V.; Gorodtsov, V.A.; Lisovenko, D.S. Auxetic mechanics of crystalline materials. *Mech. Solids* **2010**, *45*, 529–545. [[CrossRef](#)]
4. Nelson, D.F. (Ed.) Second and Higher Order Elastic Constants. In *Landolt-Börnstein—Group III Condensed Matter*; Springer: Berlin/Heidelberg, Germany, 1992; Volume 29a. [[CrossRef](#)]
5. Ting, T.C.T. The stationary values of Young's modulus for monoclinic and triclinic materials. *J. Mech.* **2005**, *21*, 249–253. [[CrossRef](#)]
6. Ting, T.C.T. Explicit expression of the stationary values of Young's modulus and the shear modulus for anisotropic elastic materials. *J. Mech.* **2005**, *21*, 255–266. [[CrossRef](#)]
7. Norris, A.N. Extreme values of Poisson's ratio and other engineering moduli in anisotropic materials. *J. Mech. Mater. Struct.* **2006**, *1*, 793–812. [[CrossRef](#)]
8. Cazzani, A.; Rovati, M. Extrema of Young's modulus for cubic and transversely isotropic solids. *Int. J. Solids Struct.* **2003**, *40*, 1713–1744. [[CrossRef](#)]
9. Cazzani, A.; Rovati, M. Extrema of Young's modulus for elastic solids with tetragonal symmetry. *Int. J. Solids Struct.* **2005**, *42*, 5057–5096. [[CrossRef](#)]
10. Norris, A.N. Poisson's ratio in cubic materials. *Proc. Roy. Soc. A* **2006**, *462*, 3385–3405. [[CrossRef](#)]
11. Epishin, A.I.; Lisovenko, D.S. Extreme values of the Poisson's ratio of cubic crystals. *Tech. Phys.* **2016**, *61*, 1516–1524. [[CrossRef](#)]
12. Gorodtsov, V.A.; Lisovenko, D.S. Extreme values of Young's modulus and Poisson's ratio of hexagonal crystals. *Mech. Mater.* **2019**, *134*, 1–8. [[CrossRef](#)]
13. Love, A.E.H. *A Treatise on the Mathematical Theory of Elasticity*; Cambridge University Press: Cambridge, UK, 1892; Volume 1.
14. Lakes, R.S. Foam structures with a negative Poisson's ratio. *Science* **1987**, *235*, 1038–1040. [[CrossRef](#)]
15. Friis, E.A.; Lakes, R.S.; Park, J.B. Negative Poisson's ratio polymeric and metallic foams. *J. Mater. Sci.* **1988**, *23*, 4406–4414. [[CrossRef](#)]
16. Evans, K.E.; Nkansah, M.A.; Hutchinson, I.J.; Rogers, S.C. Molecular network design. *Nature* **1991**, *353*, 124. [[CrossRef](#)]
17. Evans, K.E. Auxetic polymers: A new range of materials. *Endeavour* **1991**, *15*, 170–174. [[CrossRef](#)]
18. Wojciechowski, K.W. Constant thermodynamic tension Monte Carlo studies of elastic properties of a two-dimensional system of hard cyclic hexamers. *Mol. Phys.* **1987**, *61*, 1247–1258. [[CrossRef](#)]
19. Wojciechowski, K.W. Two-dimensional isotropic system with a negative Poisson ratio. *Phys. Lett. A* **1989**, *137*, 60–64. [[CrossRef](#)]

20. Tretiakov, K.V.; Wojciechowski, K.W. Poisson's ratio of simple planar 'isotropic' solids in two dimensions. *Phys. Status Solidi B* **2007**, *244*, 1038–1046. [[CrossRef](#)]
21. Tretiakov, K.V.; Wojciechowski, K.W. Auxetic, partially auxetic, and nonauxetic behaviour in 2D crystals of hard cyclic tetramers. *Phys. Status Solidi RRL* **2020**, *14*, 2000198. [[CrossRef](#)]
22. Wojciechowski, K.W.; Brańka, A.C. Negative Poisson ratio in a two-dimensional "isotropic" solid. *Phys. Rev. A* **1989**, *40*, 7222–7225. [[CrossRef](#)]
23. Wojciechowski, K.W. Non-chiral, molecular model of negative Poisson ratio in two dimensions. *J. Phys. A* **2003**, *36*, 11765–11778. [[CrossRef](#)]
24. Narojczyk, J.W.; Kowalik, M.; Wojciechowski, K.W. Influence of nanochannels on Poisson's ratio of degenerate crystal of hard dimers. *Phys. Status Solidi B* **2016**, *253*, 1324–1330. [[CrossRef](#)]
25. Tretiakov, K.V.; Pigłowski, P.M.; Hyzorek, K.; Wojciechowski, K.W. Enhanced auxeticity in Yukawa systems due to introduction of nanochannels in [001]-direction. *Smart Mater. Struct.* **2016**, *25*, 054007. [[CrossRef](#)]
26. Pigłowski, P.M.; Wojciechowski, K.W.; Tretiakov, K.V. Partial auxeticity induced by nanoslits in the Yukawa crystal. *Phys. Status Solidi RRL* **2016**, *10*, 566–569. [[CrossRef](#)]
27. Pigłowski, P.; Narojczyk, J.; Poźniak, A.; Wojciechowski, K.; Tretiakov, K. Auxeticity of Yukawa systems with nanolayers in the (111) crystallographic plane. *Materials* **2017**, *10*, 1338. [[CrossRef](#)]
28. Tretiakov, K.; Pigłowski, P.; Narojczyk, J.; Bilski, M.; Wojciechowski, K. High partial auxeticity Induced by nanochannels in [111]-direction in a simple model with Yukawa interactions. *Materials* **2018**, *11*, 2550. [[CrossRef](#)]
29. Tretiakov, K.V.; Pigłowski, P.M.; Narojczyk, J.W.; Wojciechowski, K.W. Selective enhancement of auxeticity through changing a diameter of nanochannels in Yukawa systems. *Smart Mater. Struct.* **2018**, *27*, 115021. [[CrossRef](#)]
30. Narojczyk, J.W.; Wojciechowski, K.W.; Tretiakov, K.V.; Smardzewski, J.; Scarpa, F.; Pigłowski, P.M.; Kowalik, M.; Imre, A.R.; Bilski, M. Auxetic properties of a f.c.c. crystal of hard spheres with an array of [001]-nanochannels filled by hard spheres of another diameter. *Phys. Status Solidi B* **2019**, *256*, 1800611. [[CrossRef](#)]
31. Narojczyk, J.; Wojciechowski, K. Poisson's ratio of the f.c.c. hard sphere crystals with periodically stacked (001)-nanolayers of hard spheres of another diameter. *Materials* **2019**, *12*, 700. [[CrossRef](#)]
32. Narojczyk, J.W.; Wojciechowski, K.W.; Smardzewski, J.; Imre, A.R.; Grima, J.N.; Bilski, M. Cancellation of auxetic properties in f.c.c. hard sphere crystals by hybrid layer-channel nanoinclusions filled by hard spheres of another diameter. *Materials* **2021**, *14*, 3008. [[CrossRef](#)]
33. Grima, J.N.; Evans, K.E. Auxetic behavior from rotating squares. *J. Mater. Sci. Lett.* **2000**, *19*, 1563–1565. [[CrossRef](#)]
34. Grima, J.N.; Jackson, R.; Alderson, A.; Evans, K.E. Do zeolites have negative Poisson's ratios? *Adv. Mater.* **2000**, *12*, 1912–1918. [[CrossRef](#)]
35. Grima, J.N.; Evans, K.E. Self expanding molecular networks. *Chem. Commun.* **2000**, 1531–1532. [[CrossRef](#)]
36. Grima, J.N.; Alderson, A.; Evans, K.E. Negative Poisson's ratios from rotating rectangles. *Comput. Methods Sci. Technol.* **2004**, *10*, 137–145. [[CrossRef](#)]
37. Grima, J.N.; Alderson, A.; Evans, K.E. Auxetic behaviour from rotating rigid units. *Phys. Status Solidi B* **2005**, *242*, 561–575. [[CrossRef](#)]
38. Grima, J.N.; Gatt, R.; Alderson, A.; Evans, K.E. On the potential of connected stars as auxetic systems. *Molec. Simul.* **2005**, *31*, 925–935. [[CrossRef](#)]
39. Grima, J.N.; Gatt, R.; Alderson, A.; Evans, K.E. On the origin of auxetic behaviour in the silicate  $\alpha$ -cristobalite. *J. Mater. Chem.* **2005**, *15*, 4003–4005. [[CrossRef](#)]
40. Grima, J.N.; Evans, K.E. Auxetic behavior from rotating triangles. *J. Mater. Sci.* **2006**, *41*, 3193–3196. [[CrossRef](#)]
41. Grima, J.N.; Gatt, R.; Alderson, A.; Evans, K.E. An alternative explanation for the negative Poisson's ratios in  $\alpha$ -cristobalite. *Mater. Sci. Eng. A* **2006**, *423*, 219–224. [[CrossRef](#)]
42. Grima, J.N.; Gatt, R.; Ravirala, N.; Alderson, A.; Evans, K.E. Negative Poisson's ratios in cellular foam materials. *Mater. Sci. Eng. A* **2006**, *423*, 214–218. [[CrossRef](#)]
43. Grima, J.N.; Zammit, V.; Gatt, R.; Alderson, A.; Evans, K.E. Auxetic behaviour from rotating semi-rigid units. *Phys. Status Solidi B* **2007**, *244*, 866–882. [[CrossRef](#)]
44. Grima, J.N.; Gatt, R.; Zammit, V.; Williams, J.J.; Evans, K.E.; Alderson, A.; Walton, R.I. Natrolite: A zeolite with negative Poisson's ratios. *J. Appl. Phys.* **2007**, *101*, 086102. [[CrossRef](#)]
45. Grima, J.N.; Farrugia, P.S.; Caruana, C.; Gatt, R.; Attard, D. Auxetic behaviour from stretching connected squares. *J. Mater. Sci.* **2008**, *43*, 5962–5971. [[CrossRef](#)]
46. Attard, D.; Grima, J.N. Auxetic behaviour from rotating rhombi. *Phys. Status Solidi B* **2008**, *245*, 2395–2404. [[CrossRef](#)]
47. Grima, J.N.; Farrugia, P.S.; Gatt, R.; Attard, D. On the auxetic properties of rotating rhombi and parallelograms: A preliminary investigation. *Phys. Status Solidi B* **2008**, *245*, 521–529. [[CrossRef](#)]
48. Attard, D.; Manicaro, E.; Grima, J.N. On rotating rigid parallelograms and their potential for exhibiting auxetic behaviour. *Phys. Status Solidi B* **2009**, *246*, 2033–2044. [[CrossRef](#)]
49. Grima, J.N.; Cassar, R.N.; Gatt, R. On the effect of hydrostatic pressure on the auxetic character of NAT-type silicates. *J. Non-Cryst. Solids* **2009**, *355*, 1307–1312. [[CrossRef](#)]

50. Attard, D.; Manicaro, E.; Gatt, R.; Grima, J.N. On the properties of auxetic rotating stretching squares. *Phys. Status Solidi B* **2009**, *246*, 2045–2054. [[CrossRef](#)]
51. Grima, J.N.; Gatt, R.; Ellul, B.; Chetcuti, E. Auxetic behaviour in non-crystalline materials having star or triangular shaped perforations. *J. Non-Cryst. Solids* **2010**, *356*, 1980–1987. [[CrossRef](#)]
52. Grima, J.N.; Gatt, R. Perforated sheets exhibiting negative Poisson's ratios. *Adv. Eng. Mater.* **2010**, *12*, 460–464. [[CrossRef](#)]
53. Grima, J.N.; Manicaro, E.; Attard, D. Auxetic behaviour from connected different-sized squares and rectangles. *Proc. Roy. Soc. A* **2011**, *467*, 439–458. [[CrossRef](#)]
54. Grima, J.N.; Chetcuti, E.; Manicaro, E.; Attard, D.; Camilleri, M.; Gatt, R.; Evans, K.E. On the auxetic properties of generic rotating rigid triangles. *Proc. Roy. Soc. A* **2012**, *468*, 810–830. [[CrossRef](#)]
55. Gatt, R.; Mizzi, L.; Azzopardi, K.M.; Grima, J.N. A force-field based analysis of the deformation mechanism in  $\alpha$ -cristobalite. *Phys. Status Solidi B* **2015**, *252*, 1479–1485. [[CrossRef](#)]
56. Gatt, R.; Mizzi, L.; Azzopardi, J.I.; Azzopardi, K.M.; Attard, D.; Casha, A.; Briffa, J.; Grima, J.N. Hierarchical auxetic mechanical metamaterials. *Sci. Rep.* **2015**, *5*, 8395. [[CrossRef](#)] [[PubMed](#)]
57. Dudek, K.K.; Gatt, R.; Mizzi, L.; Dudek, M.R.; Attard, D.; Evans, K.E.; Grima, J.N. On the dynamics and control of mechanical properties of hierarchical rotating rigid unit auxetics. *Sci. Rep.* **2017**, *7*, 46529. [[CrossRef](#)] [[PubMed](#)]
58. Attard, D.; Casha, A.; Grima, J. Filtration properties of auxetics with rotating rigid units. *Materials* **2018**, *11*, 725. [[CrossRef](#)] [[PubMed](#)]
59. Evans, K.E.; Alderson, A. Rotation and dilation deformation mechanisms for auxetic behaviour in the  $\alpha$ -cristobalite tetrahedral framework structure. *Phys. Chem. Min.* **2001**, *28*, 711–718. [[CrossRef](#)]
60. Alderson, A.; Evans, K.E. Molecular origin of auxetic behavior in tetrahedral framework silicates. *Phys. Rev. Lett.* **2002**, *89*, 225503. [[CrossRef](#)]
61. Alderson, A.; Alderson, K.L.; Evans, K.E.; Grima, J.N.; Williams, M.R.; Davies, P.J. Molecular modeling of the deformation mechanisms acting in auxetic silica. *Comput. Methods Sci. Technol.* **2004**, *10*, 117–126. [[CrossRef](#)]
62. Alderson, A.; Alderson, K.L.; Evans, K.E.; Grima, J.N.; Williams, M.R.; Davies, P.J. Modelling the deformation mechanisms, structure-property relationships and applications of auxetic nanomaterials. *Phys. Status Solidi B* **2005**, *242*, 499–508. [[CrossRef](#)]
63. Alderson, A.; Alderson, K.L.; Evans, K.E.; Grima, J.N.; Williams, M.S. Modelling of negative Poisson's ratio nanomaterials: Deformation mechanisms, structure-property relationships and applications. *J. Metastab. Nanocryst. Mater.* **2005**, *23*, 55–58. [[CrossRef](#)]
64. Alderson, A.; Evans, K.E. Deformation mechanisms leading to auxetic behaviour in the  $\alpha$ -cristobalite and  $\alpha$ -quartz structures of both silica and germania. *J. Phys. Condens. Matter* **2008**, *21*, 025401. [[CrossRef](#)] [[PubMed](#)]
65. Grima, J.N.; Zammit, V.; Gatt, R.; Attard, D.; Caruana, C.; Chircop Bray, T.G. On the role of rotating tetrahedra for generating auxetic behavior in NAT and related systems. *J. Non-Cryst. Solids* **2008**, *354*, 4214–4220. [[CrossRef](#)]
66. Attard, D.; Grima, J.N. A three-dimensional rotating rigid units network exhibiting negative Poisson's ratios. *Phys. Status Solidi B* **2012**, *249*, 1330–1338. [[CrossRef](#)]
67. Azzopardi, K.M.; Brincat, J.P.; Grima, J.N.; Gatt, R. Anomalous elastic properties in stishovite. *RSC Adv.* **2015**, *5*, 8974–8980. [[CrossRef](#)]
68. Nazaré, F.; Alderson, A. Models for the prediction of Poisson's ratio in the ' $\alpha$ -cristobalite' tetrahedral framework. *Phys. Status Solidi B* **2015**, *252*, 1465–1478. [[CrossRef](#)]
69. Grima-Cornish, J.N.; Vella-Žarb, L.; Grima, J.N. Negative linear compressibility and auxeticity in boron arsenate. *Annal. Physik* **2020**, *532*, 1900550. [[CrossRef](#)]
70. Grima-Cornish, J.N.; Grima, J.N.; Attard, D. A novel mechanical metamaterial exhibiting auxetic behavior and negative compressibility. *Materials* **2020**, *13*, 79. [[CrossRef](#)]
71. Dudek, K.K.; Attard, D.; Gatt, R.; Grima-Cornish, J.N.; Grima, J.N. The multidirectional auxeticity and negative linear compressibility of a 3D mechanical metamaterial. *Materials* **2020**, *13*, 2193. [[CrossRef](#)]
72. Grima-Cornish, J.N.; Vella-Žarb, L.; Wojciechowski, K.W.; Grima, J.N. Shearing deformations of  $\beta$ -cristobalite-like boron arsenate. *Symmetry* **2021**, *13*, 977. [[CrossRef](#)]
73. Milstein, F.; Huang, K. Existence of a negative Poisson ratio in fcc crystals. *Phys. Rev. B* **1979**, *19*, 2030–2033. [[CrossRef](#)]
74. Baughman, R.H.; Shacklette, J.M.; Zakhidov, A.A.; Stafström, S. Negative Poisson's ratios as a common feature of cubic metals. *Nature* **1998**, *392*, 362–365. [[CrossRef](#)]
75. Paszkiewicz, T.; Pruchnik, M.; Wolski, S. Slowness surfaces and energy focusing patterns of auxetic cubic media. *Comput. Methods Sci. Technol.* **2004**, *10*, 183–195. [[CrossRef](#)]
76. Paszkiewicz, T.; Wolski, S. Anisotropic properties of mechanical characteristics and auxeticity of cubic crystalline media. *Phys. Status Solidi B* **2007**, *244*, 966–977. [[CrossRef](#)]
77. Paszkiewicz, T.; Wolski, S. Elastic properties of cubic crystals: Every's versus Blackman's diagram. *J. Phys. Conf. Ser.* **2008**, *104*, 012038. [[CrossRef](#)]
78. Jasiukiewicz, C.; Paszkiewicz, T.; Wolski, S. Auxetic properties and anisotropy of elastic material constants of 2D crystalline media. *Phys. Status Solidi B* **2008**, *245*, 562–569. [[CrossRef](#)]
79. Brańka, A.C.; Wojciechowski, K.W. Auxeticity of cubic materials: The role of repulsive core interaction. *J. Non-Cryst. Solids* **2008**, *354*, 4143–4145. [[CrossRef](#)]

80. Branka, A.C.; Heyes, D.M.; Wojciechowski, K.W. Auxeticity of cubic materials. *Phys. Status Solidi B* **2009**, *246*, 2063–2071. [[CrossRef](#)]
81. Branka, A.C.; Heyes, D.M.; Wojciechowski, K.W. Auxeticity of cubic materials under pressure. *Phys. Status Solidi B* **2011**, *248*, 96–104. [[CrossRef](#)]
82. Branka, A.C.; Heyes, D.M.; Maćkowiak, S.; Pieprzyk, S.; Wojciechowski, K.W. Cubic materials in different auxetic regions: Linking microscopic to macroscopic formulations. *Phys. Status Solidi B* **2012**, *249*, 1373–1378. [[CrossRef](#)]
83. Goldstein, R.V.; Gorodtsov, V.A.; Lisovenko, D.S. Cubic auxetics. *Dokl. Phys.* **2011**, *56*, 399–402. [[CrossRef](#)]
84. Goldstein, R.V.; Gorodtsov, V.A.; Lisovenko, D.S. Relation of Poisson's ratio on average with Young's modulus. Auxetics on average. *Dokl. Phys.* **2012**, *57*, 174–178. [[CrossRef](#)]
85. Goldstein, R.V.; Gorodtsov, V.A.; Lisovenko, D.S. Classification of cubic auxetics. *Phys. Status Solidi B* **2013**, *250*, 2038–2043. [[CrossRef](#)]
86. Goldstein, R.V.; Gorodtsov, V.A.; Lisovenko, D.S.; Volkov, M.A. Negative Poisson's ratio for cubic crystals and nano/microtubes. *Phys. Mesomech.* **2014**, *17*, 97–115. [[CrossRef](#)]
87. Krasavin, V.V.; Krasavin, A.V. Auxetic properties of cubic metal single crystals. *Phys. Status Solidi B* **2014**, *251*, 2314–2320. [[CrossRef](#)]
88. Ho, D.T.; Park, S.D.; Kwon, S.Y.; Park, K.; Kim, S.Y. Negative Poisson's ratios in metal nanoplates. *Nat. Commun.* **2014**, *5*, 3255. [[CrossRef](#)]
89. Ho, D.T.; Kim, H.; Kwon, S.Y.; Kim, S.Y. Auxeticity of face-centered cubic metal (001) nanoplates. *Phys. Status Solidi B* **2015**, *252*, 1492–1501. [[CrossRef](#)]
90. Ho, D.T.; Park, S.D.; Kwon, S.Y.; Han, T.S.; Kim, S.Y. Negative Poisson's ratio in cubic materials along principal directions. *Phys. Status Solidi B* **2016**, *253*, 1288–1294. [[CrossRef](#)]
91. Goldstein, R.V.; Gorodtsov, V.A.; Lisovenko, D.S.; Volkov, M.A. Two-layer tubes from cubic crystals. *Dokl. Phys.* **2016**, *61*, 604–610. [[CrossRef](#)]
92. Lisovenko, D.S.; Baimova, J.A.; Rysaeva, L.K.; Gorodtsov, V.A.; Rudskoy, A.I.; Dmitriev, S.V. Equilibrium diamond-like carbon nanostructures with cubic anisotropy: Elastic properties. *Phys. Status Solidi B* **2016**, *253*, 1295–1302. [[CrossRef](#)]
93. Goldstein, R.V.; Gorodtsov, V.A.; Lisovenko, D.S.; Volkov, M.A. Two-layered tubes from cubic crystals: Auxetic tubes. *Phys. Status Solidi B* **2017**, *254*, 1600815. [[CrossRef](#)]
94. Lisovenko, D.S.; Baimova, Y.A.; Rysaeva, L.K.; Gorodtsov, V.A.; Dmitriev, S.V. Equilibrium structures of carbon diamond-like clusters and their elastic properties. *Phys. Solid State* **2017**, *59*, 820–828. [[CrossRef](#)]
95. Goldstein, R.V.; Gorodtsov, V.A.; Lisovenko, D.S. Longitudinal elastic tension of two-layered plates from isotropic auxetics-nonauxetics and cubic crystals. *Eur. J. Mech. A Solids* **2017**, *63*, 122–127. [[CrossRef](#)]
96. Gorodtsov, V.A.; Lisovenko, D.S.; Lim, T.C. Three-layered plate exhibiting auxeticity based on stretching and bending modes. *Compos. Struct.* **2018**, *194*, 643–651. [[CrossRef](#)]
97. Rysaeva, L.K.; Baimova, J.A.; Lisovenko, D.S.; Gorodtsov, V.A.; Dmitriev, S.V. Elastic properties of fullerenes and diamond-like phases. *Phys. Status Solidi B* **2019**, *256*, 1800049. [[CrossRef](#)]
98. Goldstein, R.V.; Gorodtsov, V.A.; Lisovenko, D.S.; Volkov, M.A. Thin homogeneous two-layered plates of cubic crystals with different layer orientation. *Phys. Mesomech.* **2019**, *22*, 261–268. [[CrossRef](#)]
99. Bryukhanov, I.A.; Gorodtsov, V.A.; Lisovenko, D.S. Chiral Fe nanotubes with both negative Poisson's ratio and Poynting's effect. Atomistic simulation. *J. Phys. Cond. Matt.* **2019**, *31*, 475304. [[CrossRef](#)] [[PubMed](#)]
100. Bryukhanov, I.A.; Gorodtsov, V.A.; Lisovenko, D.S. Modeling of the mechanical properties of chiral metallic nanotubes. *Phys. Mesomech.* **2020**, *23*, 477–486. [[CrossRef](#)]
101. Bielejewska, N.; Brańka, A.C.; Pieprzyk, S.; Yevchenko, T. Another look at auxeticity of 2D square media. *Phys. Status Solidi B* **2020**, *257*, 2000485. [[CrossRef](#)]
102. Gorodtsov, V.A.; Lisovenko, D.S. Auxetics among materials with cubic anisotropy. *Mech. Solids* **2020**, *55*, 461–474. [[CrossRef](#)]
103. Volkov, M.A.; Gorodtsov, V.A.; Fadeev, E.P.; Lisovenko, D.S. Stretching of chiral tubes obtained by rolling-up plates of cubic crystals with various orientations. *J. Mech. Mater. Struct.* **2021**, *16*, 139–157. [[CrossRef](#)]
104. Sirotnin, Y.I.; Shaskolskaya, M.P. *Fundamentals of Crystal Physics*; Mir: Moscow, Russia, 1982.
105. Nye, J.F. *Physical Properties of Crystals*; Clarendon Press: Oxford, UK, 1957; 329p.
106. Goldstein, R.V.; Gorodtsov, V.A.; Lisovenko, D.S. Young's modulus of cubic auxetics. *Lett. Mater.* **2011**, *1*, 127–132. [[CrossRef](#)]
107. Smirnov, V.I. *A Course of Higher Mathematics, Vol. I: Elementary Calculus*; Pergamon Press: Oxford, UK, 1964; 546p.
108. Gorodtsov, V.A.; Tkachenko, V.G.; Lisovenko, D.S. Extreme values of Young's modulus of tetragonal crystals. *Mech. Mater.* **2021**, *154*, 103724. [[CrossRef](#)]
109. Goldstein, R.V.; Gorodtsov, V.A.; Lisovenko, D.S.; Volkov, M.A. Auxetics among 6-constant tetragonal crystals. *Lett. Mater.* **2015**, *5*, 409–413. [[CrossRef](#)]